

The design and test of MEMS piezoresistive ultrasonic sensor arrays*

Lian Deqin(廉德钦)^{1,2,†}, He Changde(何常德)^{1,2}, Zhang Hui(张慧)¹, Yu Jiaqi(于佳琪)¹,
Yuan Kejing(宛克敬)², and Xue Chenyang(薛晨阳)^{1,2}

¹Key Laboratory of Instrumentation Science & Dynamic Measurement, Ministry of Education, North University of China, Taiyuan 030051, China

²Key Laboratory of Science and Technology on Electronic Test & Measurement, North University of China, Taiyuan 030051, China

Abstract: The design, fabrication and packaging of a type of MEMS piezoresistive ultrasonic transducer array are introduced. The consistency of the resonance frequency and the sensitivity of the array are tested. Moreover, we detect the directivity and the multi-target identification ability of the array. The results of the consistency of the resonance frequency and the sensitivity show that there is a gap between the practical and theoretical results. This paper analyzes this problem in detail and points out the direction of improvement. As for the directivity, the actual result is consistent with the theoretical one. The results of multiple target distinguishing tests demonstrate that the smallest resolution angle of the array is 5.72° when the distance between the sensor array and measured objects is 2 m.

Key words: ultrasonic sensor; piezoresistive; integrated array; multi-target identification

DOI: 10.1088/1674-4926/34/3/034007 **EEACC:** 2570

1. Introduction

Ultrasonic imaging systems have been widely applied in the fields of medicine and sonar. In addition, the B-ultrasound has been widely used for disease diagnosis. Sonar data visualization technology plays an indispensable role in the underwater acoustic field. It transforms a large amount of boring data into vivid images, which enable people to analyze the sonar data visually and improve the efficiency of underwater detection. As the key part of the electric sound conversion system, the ultrasonic sensor's material and structure have been a research focus. The MEMS ultrasonic sensor has the advantage of being able to be arrayed and has higher frequency when comparing with traditional ones. In addition, it has obvious advantages in the pursuit for high precision and IC integration processes^[1]. Three types of ultrasonic sensor are now being studied, piezoelectric, capacitive, and piezoresistive. Piezoelectric sensors are more mature, and capacitive ones are the research hotspot right now. There is an extensive application of piezoresistive sensors on MEMS accelerometers and dynamometers, but rarely on acoustic sensors^[2, 3].

The North University of China (NUC) has done some research on piezoresistive low frequency acoustic sensors, and made some headway^[4]. In the field of high frequency acoustic sensors, NUC designed a “membrane-beam” structure^[5]. It is composed of two small side beams and a rectangular membrane with both ends fixed. Two resistances are placed in the middle of the membrane, and two on each side beam. The four resistances form the Wheatstone bridge. The design has solved

the problem of the temperature drift and takes advantage of the opposite stress at the same time, which has improved the sensor's sensitivity to a certain extent. The varistor value is 2 kΩ and a 2 V voltage is applied across Wheatstone bridge. Under 1 μPa pressure, the varistor value changes by 1.22×10^{-2} Ω and the output voltage is 7.88 μV. The structure is shown in Fig. 1. The test results show that the sensitivity of the new structure has been increased by 8.9 dB on average compared with the cantilever structure. With the development of MEMS process technology, the piezoresistive ultrasonic sensor will have definite application prospects due to its advantages of good compatibility with CMOS technology and simple process.

The ultrasonic sensor array is an important part of an ultrasonic imaging system. A traditional sensor array is usually large in size for it includes some relatively large sensors. Its high cost is another obstacle. Therefore, ultrasonic sensor arrays with high integration density and performance is the main direction of future research. Based on a silicon semiconductor, the MEMS piezoresistive ultrasonic sensor has the advantages of a micro piezoresistor and an integrated amplifier circuit^[6].

Following the NUC's research on the piezoresistive ultrasonic sensor, this paper focus on the application of the sensor array, anatomizes the parameters of the array, including array length, number, and spacing of array element, and processes a batch of sensor arrays with different resonant frequencies by using bulk silicon micromachining technology. The arrays are proved to have achieved the expected effect, and have the ability of multiple target resolution. The design, fabrication, and

* Project supported by the National High Technology Research and Development Program of China (No. 2011AA040404) and the Special Fund of the National Natural Science Foundation of China (No. 61127008)

† Corresponding author. Email: ldq528@163.com

Received 14 November 2012, revised manuscript received 18 December 2012

© 2013 Chinese Institute of Electronics

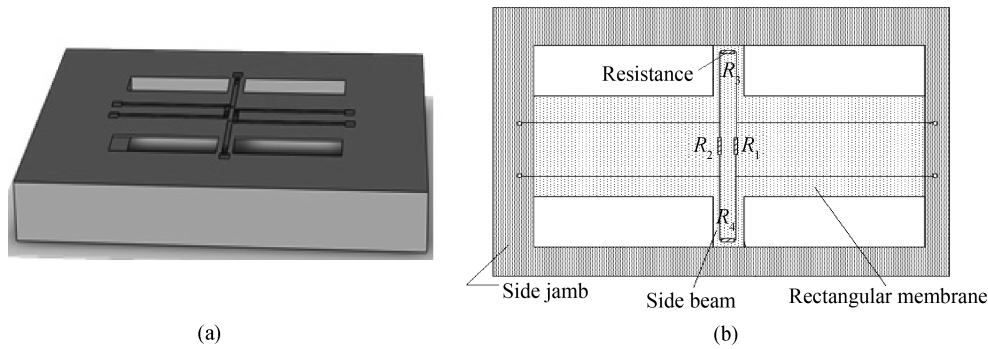


Fig. 1. The structure of the sensor. (a) Whole structure. (b) Varistor distribution of the sensing structure.

test process are as follows.

2. Design of the MEMS piezoresistive ultrasonic sensor array

From an acoustic point of view, an array of reasonable structure and good acoustic properties should be designed to avoid producing pseudo-images; otherwise there will be side lobes with strong sound intensity and even grating lobes. Consequently, pursuing a high-performance acoustic sensor array becomes the main task of the design.

2.1. The element spacing analysis

Element spacing is a basic parameter of an acoustic array; larger element spacing can improve the resolution of the array, but excessive spacing will lead to grating lobes with big energy being produced, which are not wanted during scanning and are the main cause of pseudo-images. According to the continuous wave (CW) theory, the upper critical value d_{cr} of the phase-controlled array's element spacing can be formulized as follows^[7]:

$$d_{cr} = \frac{\lambda}{1 + |\sin(\theta_s)_{\max}|}, \quad (1)$$

where $(\theta_s)_{\max}$ is the allowed maximum deflection angle at which no grating lobes are produced.

However, as a matter of fact, grating lobes cannot be eliminated completely while the element spacing is less than d_{cr} . In order to completely get rid of it, the calculation formula should be optimized as follows^[8]:

$$d_{\max} = \frac{\lambda}{1 + |\sin(\theta_s)_{\max}|} \frac{N - 1}{N}. \quad (2)$$

The maximum element spacing is the function of the maximum deflection angle. N is the number of elements. When N is large enough, the conclusion is $\lambda/2 \leq d_{\max} \leq \lambda$. And for a phase-controlled array with a few elements, the d_{\max} is decided by Eq. (2). In some instances, it may be shorter than half wavelength. Otherwise, grating lobes will be produced.

2.2. Design principles and methods of integrated arrays

To design the phase-controlled array ultrasonic sensor, firstly, the array's size is decided based on the required lateral resolution and near field length. The element spacing length is

decided based on the condition of the eliminating grating lobes. In addition, the size of the elements is determined based on the principle of maximizing the sound pressure on deflecting direction. Finally, based on the aperture of the array and the distance of element spacing, the number of elements is figured out. Generally, according to above principles, an array with enough elements and appropriate spacing can restrain the side lobes to a certain extent. From Eq. (2), it can be concluded that: if the element spacing is shorter than half of wavelength, no grating lobe will be produced. The resonant frequency of the designed ultrasonic sensor is 68 kHz and the corresponding wavelength is 5 mm. The distance between every element is half of wavelength, which is 2.5 mm. Considering that the research of processing is still at an exploratory stage, to increase the success rate of processing and ensure a firm chip, the total length of the array is designed to be 5 cm with only 9 elements in it.

3. Process and package technology of the sensor array

The process and package of an integrated ultrasonic sensor are significant research which directly restricts the performance and integration level of the sensor. On the basis of previous research, we have improved the process technology and explored the backside deep etching technology. To ensure the good acoustic performance and reliability of the designed sensor, the package technology of MEMS ultrasonic sensors should also be taken seriously.

3.1. Process technology of the sensor array

As bulk silicon micromachining technology costs less than sacrificial layers technology^[9] and is a mature technology in China, we use it to process the integrated ultrasonic sensor array. In order to process the membrane at a proper thickness, we need to apply backside deep etching technology. SOI (crystal orientation: (100); resistivity: 2–4 Ω·cm; thickness: $20 \pm 1 \mu\text{m}$) is a good choice for its advantage that the SiO_2 in the middle layer will be an etch stop layer, which means that the etching depth can be well controlled while applying backside deep etching. The main fabrication process is shown in Fig. 2: (a) high temperature oxidization of the top silicon, the oxide thicknesses is 1000 Å; (b) create the resistor bar window by RIE etching; (c) produce the resistance via boron doping, concentration of boron: $4 \times 10^{18} \text{ cm}^{-3}$; (d) oxidize the top again, and

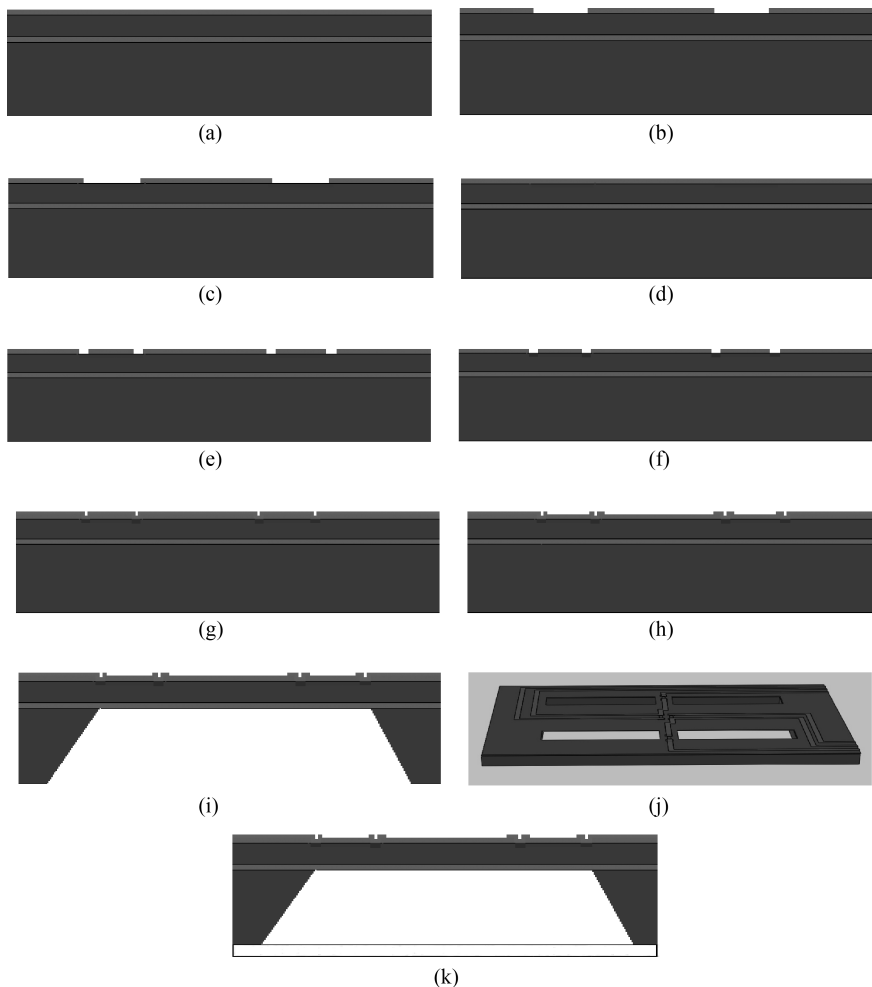


Fig. 2. The process steps of ultrasonic sensors.

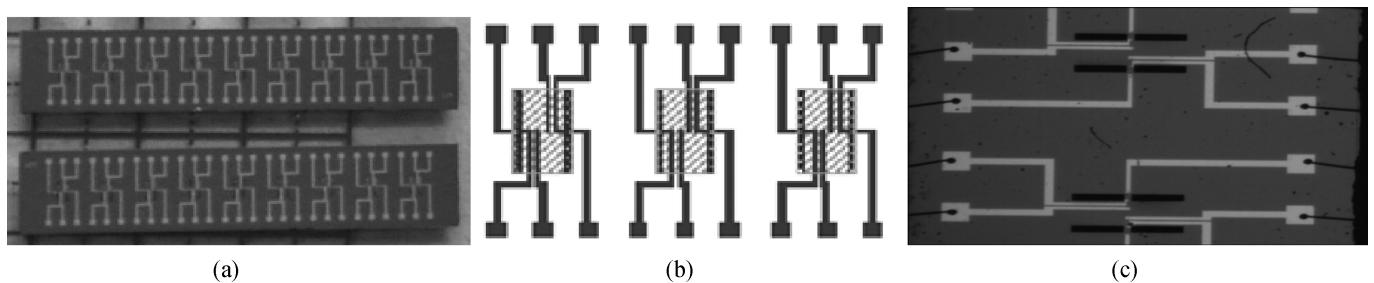


Fig. 3. The finished sensor array. (a) Sensor arrays. (b) Local amplification image. (c) The scanning electron microscope.

isolate the resistance from air contact; (e) RIE etching, etching area for diffusion concentration of boron, used for metal contact; (f) heavy boron doping, then oxidize the top again, formation of the electrode hole by RIE etching; (g) deposition of metal by thermal evaporation: first Cr, 500 Å, then Au, 1000 Å; (h) unnecessary metal removed to produce a metal wire; (i) etching on backside: ICP technology; (j) etching on obverse side: ICP technology; RIE etching: SiO₂ was etched on the back side; (k) bonding glass to the substrate: glass was bonded to the substrate using anodic bonding technology.

After designing some cells by using the above fabrication process, linear arrays with different resonance frequency are designed and manufactured as shown in Fig. 3.

3.2. Package of the sensor array

Generally, the sensing unit is sealed when packaging the MEMS device. However, for the acoustic sensor, a different package method is applied. Since the sensing unit of the acoustic sensor needs to be in contact with the sound transmission medium, some problems, such as sound transmission ability, external and internal disturbance, the stability of the structure and how to shorten the wires with the following amplifying circuit, should be paid attention while packaging the chips. So the package of the multilayer PCB structure is designed to be double-layer metal-coated and to have wires in the middle layer.

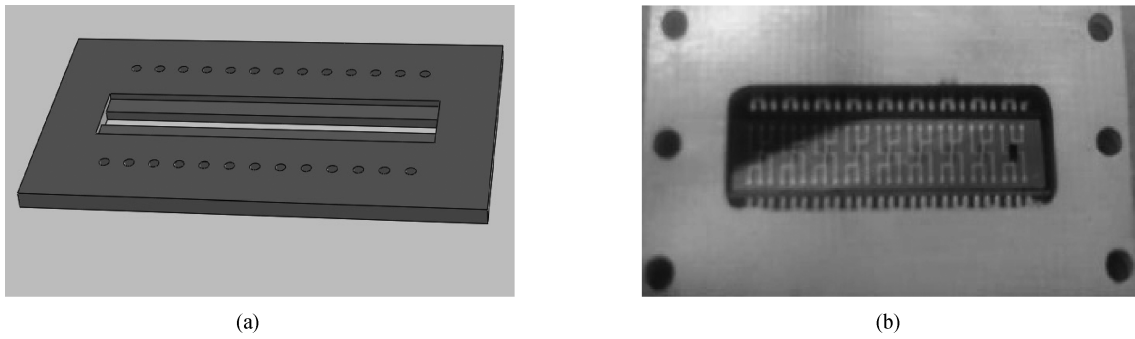


Fig. 4. Packaging of the sensor array. (a) The machine drawing of packaging. (b) The packaged chip.

Table 1. Testing results of the linear array's resonance frequency.

Element serial number	1	2	3	4	5	6	7	8	9
NO.1 array (kHz)	43	43.6	44	45	46	46	46	45	44
NO.2 array (kHz)	51.9	51.8	51.3	51.4	51.4	51.4	51.4	52.6	51.8

As shown in Fig. 4(a), the chip is glued to the perforated baseplate. The holes on the baseplate can reduce the damping effect of air and improve the sensor's sensitivity. A metal welding pad is designed for connection to the PCB by gold bonding. Since the chip is exposed in the air, a steel mesh on the frame is applied to protect the sensing unit from mechanical damage. The package process only accomplishes the connection with the circuit board and basic protection of the chip, and in actual application, a crust is also required for the chip's security. Figure 4(b) shows the packaged chip.

4. Test of the sensor array's performance

4.1. Test of the consistency of the resonance frequency

Unlike a low frequency acoustic sensor, which works at half of the resonance frequency, the ultrasonic sensor's working frequency is almost the resonance frequency. By emitting sound waves of different frequency, the ultrasonic sensor's maximum response is tested, where the frequency is right at the resonance frequency. The test result of the piezoresistive sensor array's resonance frequency is shown in Table 1.

The NO.1 linear array's expectation and variance^[10]:

$$E_w = \frac{1}{9} \sum_{i=1}^9 w_i = 44.7 \text{ K},$$

$$S_w = \frac{1}{9-1} \sum_{i=1}^9 (x_i - E_w)^2 = 1.29 \text{ K}^2.$$

The NO.2 linear array expectation and variance:

$$E_w = \frac{1}{9} \sum_{i=1}^9 w_i = 51.7 \text{ K},$$

$$S_w = \frac{1}{9-1} \sum_{i=1}^9 (x_i - E_w)^2 = 0.173 \text{ K}^2.$$

w represents the resonance frequency here.

As the table shows, the consistency of the resonance frequency is good for the elements in the same array, but is obviously different between the two arrays. Meanwhile, some issues lead to the situation that the actual result is dissimilar to the theory. (1) The top silicon of the SOI is uneven in thickness. (2) The elastic modulus of the silicon is different in simulation and practice. (3) The etching process is not controlled well, so the depth is not same with expected. (4) The residual stress inside the structure results in a different resonance frequency from the actual data and from the theoretical expectation. So process practice and design improvements are required in order to produce an ultrasonic sensor array with good performance.

4.2. Test of the consistency of the sensitivity

This paper uses the voltage sensitivity as an indicator. M_e is the pressure sensitivity, e_{oc} is the open-circuit voltage of the sensor and p_i is the sound pressure prior to placing the sensor. The relation between them is:

$$M_e = \frac{e_{oc}}{p_i}, \quad (3)$$

where the unit of e_{oc} is V, P_i is μPa , and M_e is $\text{V}/\mu\text{Pa}$. For a vector ultrasonic sensor, the sound pressure sensitivity is associated with the direction of the plane wave relative to the sensor. M_{el} is the voltage sensitivity and its unit is decibel (dB). It can be expressed as follows:

$$M_{el} = 20 \lg \frac{M_e}{M_{e0}}. \quad (4)$$

The voltage sensitivity value is based on M_{e0} , which is usually valued: $M_{e0} = 1 \text{ V}/\mu\text{Pa}$. The piezoresistive ultrasonic sensor is based on the Wheatstone bridge. A load of $1 \mu\text{Pa}$ is applied. The sensor's resistance changes, which results in imbalance of the bridge and produces a voltage change Δu and $M_e = \Delta u/1 \mu\text{Pa}$. The result of a linear array's sensitivity test is shown in Table 2.

The NO. 1 linear array's expectation and variance:

$$E_{M_{el}} = \frac{1}{9} \sum_{i=1}^9 (M_{el})_i = -202.7 \text{ dB},$$

Table 2. The result of a linear array's sensitivity level test.

Element serial number	1	2	3	4	5	6	7	8	9
NO.1 array (dB)	-202	-200	-200.6	-203	-203.2	-205.4	-203	-202.7	-203.8
NO.2 array (dB)	-206	-203	-203.3	-205	-205.4	-205.4	-201.8	-201.2	-205.1

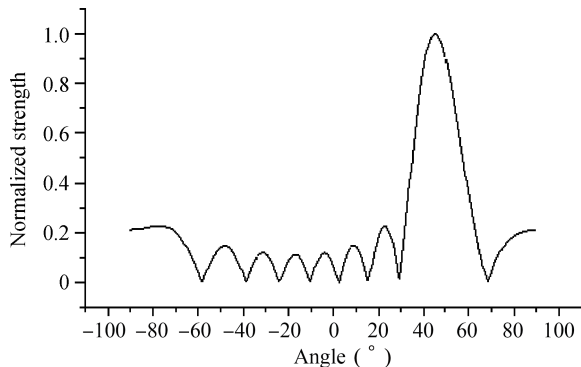


Fig. 5. The normalized directivity of the array.

$$S_{M_{el}} = \frac{1}{9-1} \sum_{i=1}^9 (M_{el} - E_{M_{el}})^2 = 2.18 \text{ dB}^2.$$

The NO. 2 linear array's expectation and variance:

$$E_{M_{el}} = \frac{1}{9} \sum_{i=1}^9 (M_{el})_i = -204.1 \text{ dB},$$

$$S_{M_{el}} = \frac{1}{9-1} \sum_{i=1}^9 (M_{el} - E_{M_{el}})^2 = 2.89 \text{ dB}^2.$$

4.3. Test of the sensor array's directivity

The directivity of the sensor array is that the sensor gathers the signals coming from different directions to one direction via phase-shift technology, and then gets the strength value of the beam. Suppose that $I(x)$ represents the strength of the sensor's directivity; the function of the sensor array's directivity can be expressed as follows:

$$G(\theta) = I(\theta) \frac{\sin\left(\frac{N}{2}\phi\right)}{N \sin\left(\frac{1}{2}\phi\right)} = I(\theta) \frac{\sin\left(\frac{N\pi d}{\lambda} \sin\theta\right)}{N \sin\left(\frac{\pi d}{\lambda} \sin\theta\right)}. \quad (5)$$

If the main direction of the array is θ_0 , the directivity function will be:

$$G(\theta) = I(\theta) \frac{\sin\left[\frac{N\pi d}{\lambda} (\sin\theta - \sin\theta_0)\right]}{N \sin\left(\frac{\pi d}{\lambda} (\sin\theta - \sin\theta_0)\right)}. \quad (6)$$

Generally, the normalized directivity of the acoustic sensor unit with a membrane structure can meet the following relation: $I(\theta) = \cos\theta$. The theoretical normalized directivity pattern is shown in Fig. 5, when parameters meet the conditions: $\theta_0 = \pi/4$, $N = 9$, $d = \lambda/2$.

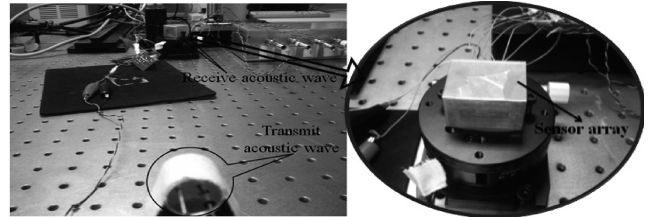


Fig. 6. The test site of the sensor array's directivity test.

In the test, an amplifying circuit with a 1000 times magnification is used. A 40 kHz ultrasonic probe is used as an ultrasonic transmitter to launch sound, which is connected to a signal generator on the positive and negative pole. The signal generator generates a 10 V signal that makes the probe produce sound of 20 Pa at a distance of 10 cm. The ultrasonic transmitter is fixed on an experimental table and the sensor array on an angle regulation stent which can be rotated within 360°. To ensure the distance between the array and the ultrasonic transmitter is constant, the sensor array is fixed on the centre of the stent's spindle. The ultrasonic transmitter launches ultrasonic waves and then rotates the stent equidistantly. The data is recorded at every angle, and the test site is shown in Fig. 6.

If we collect 9 groups of signals simultaneously, this will lead to a great amount of data. So, to reduce the data acquisition quantity and meet the digital beam-forming conditions, 4 sampling sites are collected in one period of each signal. In order to achieve the phase shift of any angle, we estimate the phase of any site located between each two sampling sites by using the two point estimation method. Suppose that a sampling site is expressed as $\sin(wt + \phi)$, the following one's phase is 90° different from it. So it can be expressed as $\cos(wt + \phi) = \sin(wt + \phi + 90^\circ)$. Any site between the two sampling sites can be estimated by the following formula:

$$\begin{aligned} \sin(wt + \phi + \Delta\phi) &= \sin(wt + \phi) \cos(\Delta\phi) \\ &\quad + \cos(wt + \phi) \sin(\Delta\phi). \end{aligned} \quad (7)$$

To deal with the 9 group of signals collected by the sensor, each signal's phase shift should be moved and superposed in order to form a beam on a particular direction. According to different delay situations, different beams are formed. Based on the direction and the corresponding beam strength, the array's directivity can be obtained ultimately. The function graph is shown in Fig. 7.

4.4. Test of the sensor array's multi-objective identification

The array's resolution angle is the allowed minimum angle between two objectives which can be distinguished. Once the angle is smaller than the resolution angle, the objectives will be regarded as a whole. The test process is as follows: firstly, generate a high-frequency pulse ultrasonic wave with a time

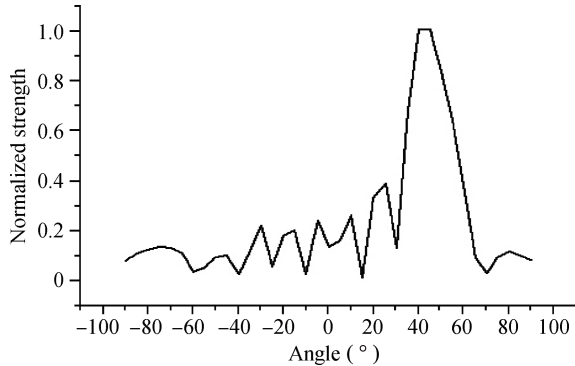


Fig. 7. The actual result of the array's directivity test.

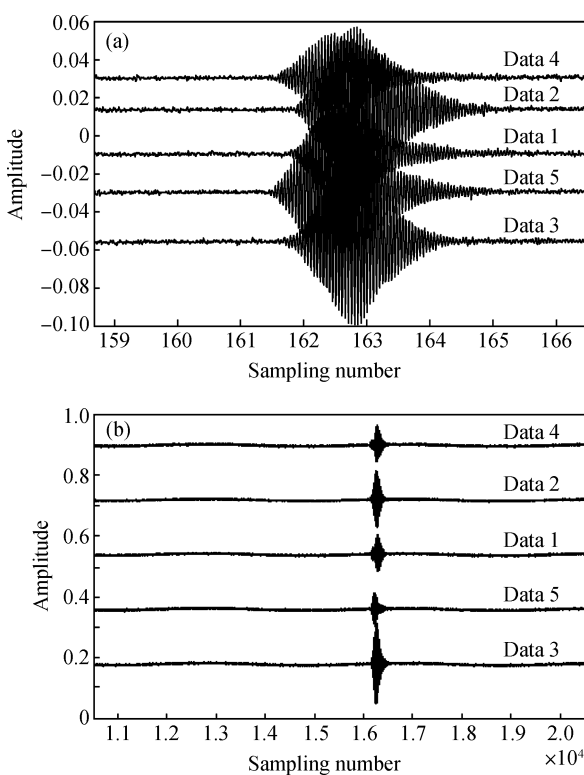


Fig. 8. Target discrimination. (a) The 5 group of signals. (b) The 5 beams.

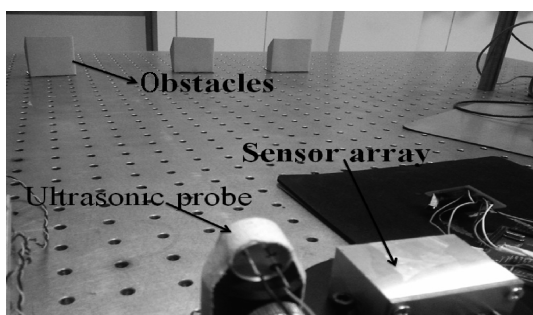


Fig. 9. The test site of the minimum angle of resolution.

interval recorded as t_0 by a pulse generator and the ultrasonic probe, and then place some obstacles optionally in the signal area. The sensor array will collect the reflected signals. The

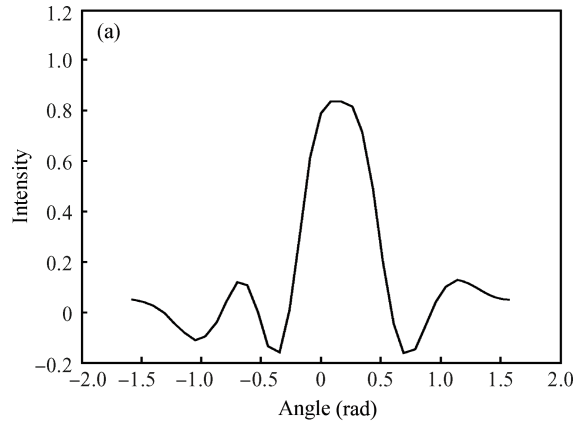


Fig. 10. Multi-objective identification. (a) Less than MAR. (b) Larger than MAR. (c) The resolution for 3 targets.

direction of obstacles can be judged via phase shifts and superposition. By calculating the time lag Δt between the launched signals and received signals, the distance can be figured out by formula $d = \Delta t \cdot c/2$.

Then the two objectives are distinguished via digital beam forming technology. Firstly, a group of 5 signals is sampled by a sampling frequency of 200 kHz. The direction right towards the sensor is taken as the normal direction, and one of the objectives is placed at 30° and the other at -45° . The group of 5 signals is shown in Fig. 8(a). The signals are then processed by digital beam forming technology. Five beams are obtained by using 5 different schemes of delay superposition, as Figure 8(b) shows. From the figure we can see that from the bottom up, beams NO. 1 and NO. 4 are stronger, which indicates that

the objects exist in these two directions. By improving the sampling frequency to form finer beams, a more accurate direction of the objects will be obtained.

Next is the test for the minimum angle of resolution (MAR). We use two $10 \times 10 \text{ cm}^2$ cardboard obstacles at a distance of 2 m from the sensor and test the resolution effect by moving them to different azimuth angles. As a result, when the distance between the two obstacles is less than 10 cm, they are confused as a whole. By applying the geometric operation, the MAR can be figured out as 5.72° when the distance between obstacles and the sensor is 2 m. Figure 9 shows the test site.

Finally, the multi-target distinguishing is tested. The phase shift superposition is applied to the group of 9 signals collected by the sensor array to form the beams. Then the energy of each beam is figured out and recorded as I . Each beam corresponds to one angle direction and is recorded as θ . Then a normalized angle-energy relationship diagram can be drawn as follows. Figure 10(a) shows only one spike because when the angle between two objectives is less than the MAR, multiple objectives will be confused as a whole. Once the angle is larger than the MAR, the sensor can distinguish each objective. Figures 10(b) and 10(c) show the results of the array's distinction for 2 and 3 objectives respectively. A low quantity of elements leads to a decrease of the array's resolution so that the sensor can only detect whether the targets exist or not, but cannot determine their size and shape. To improve the resolution we can increase the quantity of the array's elements.

5. Conclusion

This paper introduced the design, fabrication and package of an array of MEMS piezoresistive ultrasonic sensors. The consistency of resonance frequency and sensitivity, the directivity and the ability of multi-target identification of the array are presented. From the results we can draw a conclusion that the actual result of the directivity corresponds with the theory, but there is a gap between the practical and theoretical results

due to the consistency of resonance frequency and sensitivity. The results of the multi-target distinguishing test show that the smallest resolution angle of the array is 5.72° when the distance between the sensor array and measured objects is 2 ms. Therefore, it is clear that the expectation effect of the designed sensor array has been achieved, which also proves the correctness of our design process. Since the quantity of array elements is insufficient, the array's resolution is low. Therefore, optimization of the process technology and increasing the quantity of array elements to improve the resolution is the direction of our further research.

References

- [1] Zhang Jinhong, Ma Jianqiang, Li Baoqing, et al. Structure design and characterization of MEMS piezoelectric ultrasonic transducer. *Piezoelectrics & Acoust Optics*, 2010, 32(4): 604
- [2] Wang Dajun, Li Huaijiang. Design of silicon piezoresistive pressure sensor chip based on MEMS technology. *Journal of Jilin Normal University (Natural Science Edition)*, 2011, 2(2): 133
- [3] Chen Shang, Xue Chenyang, Zhang Wendong, et al. Fabrication and testing of a silicon-based piezoresistive two-axis accelerometer. *Nanotechnology and Precision Engineering*, 2008, 6(4): 272
- [4] Qiao Hui, Liu Jun, Zhang Binzen, et al. Design of a novel Si_2 based bionic vector hydrophone based on piezoresistive effect. *Chinese Journal of Sensors and Actuators*, 2008, 21(2): 301
- [5] Yuan Kejing, He Changde, Lian Deqin, et al. Designing of MEMS piezoresistive ultra transducer. *Piezoelectrics & Acoust Optics*, 2012, 34(5): 728
- [6] Zhang Huixin. Design of MEMS-based piezoresistive microcantilever biosensor. Master Thesis of Tianjin University, 2007
- [7] Wooh S C, Shi Y. Optimum beam steering of linear phased arrays. *Wave Motion*, 1999, 29: 245
- [8] Feng Ruo, Yao Jinzhong, Guan Lixun. *Ultrasonics handbook*. Nanjing University Press, 2006: 254
- [9] Wang Yangyuan, Wu Guoying, Hao Yilong, et al. Study of silicon-based MEMS technology and its standard process. *Acta Electronica Sinica*, 2002, 30(11): 1577
- [10] Wang Zhongyuan, Zhang Lingke. *Rocket general firing table and test method of trajectory consistency*. Science Press, 2008: 3